Catalysis Science & Technology

PAPER

View Article Online
View Journal | View Issue

Cite this: *Catal. Sci. Technol.*, 2015, 5, 2103

Sustainable production of dimethyl adipate by non-heme iron(III) catalysed oxidative cleavage of catechol†

Robin Jastrzebski, Emily J. van den Berg, Bert M. Weckhuysen and Pieter C. A. Bruijnincx*

Received 27th November 2014,
Accepted 15th December 2014

DOI: 10.1039/c4cy01562b

www.rsc.org/catalysis

Adipic acid and its esters are important bulk chemicals whose principal use is in the production of the nylon-6,6 polymer. There is considerable interest in finding novel green routes from sustainable feedstocks towards these important intermediates. Herein, we describe the catalytic oxidative cleavage of catechol to muconic acids using a catalyst prepared *in situ* from iron(III) nitrate, tris(2-pyridylmethyl)amine and ammonium acetate. An investigation of catalyst loading, temperature and oxygen pressure, allowed a turnover frequency of 120 h^{-1} to be obtained. The subsequent hydrogenation and transesterification of the obtained muconic acid products were shown to proceed well over commercially available supported catalysts. After vacuum distillation, dimethyl adipate could be isolated in 62% yield from catechol, thus demonstrating a green and sustainable route to this important bulk chemical.

1. Introduction

Adipic acid and its diesters are the most important carboxylic diacids produced in the chemical industry, with a production of approximately 2.8 million tons per year. The most important application is the production of the nylon-6,6 polyamide, although other uses include synthesis of polyesters and polyurethanes, plasticisers in polyvinyl chloride and polyvinyl butyral and as additives in numerous other applications.[1]

The current industrial production of adipic acid (Fig. 1) starts from oil-derived benzene, which is first hydrogenated to cyclohexane. Cyclohexane is typically oxidized by air to KA-oil, which is a mixture of cyclohexanol and cyclohexanone, over a cobalt catalyst.[2] As selectivity is inversely dependent on cyclohexane conversion, this reaction is typically run at low (4–8%) conversion and requires continuous distillation and recycling of cyclohexane.[3] Subsequent oxidation of the KA oil with nitric acid affords adipic acid, as well as a stoichiometric amount of nitrous oxide, a strong greenhouse gas.[4,5] There is considerable interest in novel processes for the production of adipic acid, both to abate waste emissions and to expand the feedstock to sustainable alternatives for benzene.

Inorganic Chemistry and Catalysis, Debye Institute for Nanomaterials Science, Utrecht University, Universiteitsweg 99, 3584 CG Utrecht, The Netherlands. E-mail: p.c.a.bruijnincx@uu.nl

† Electronic supplementary information (ESI) available: ^{1}H NMR spectra, analytical data for dimethyl adipate, absolute energies and Cartesian coordinates for calculated structures. See DOI: 10.1039/c4cy01562b

Van de Vyver and Román-Leshkov recently reviewed the development of novel catalytic processes for adipic acid production.[6] The furthest developed alternative to the current industrial production is the oxidation of cyclohexene with 30% hydrogen peroxide with a catalyst based on soluble tungstates, which was first reported by Sato *et al.*[7] Several routes starting from renewable substrates have also been reported, for example from 5-hydroxymethylfurfural,[8] γ-valerolactone[9] and D-glucose.[10] In the latter, biochemical, route *E. coli* strains were engineered to convert glucose into *cis*,*cis*-muconic acid, which could in turn be readily converted into adipic acid by catalytic hydrogenation. Lignin could also serve as a renewable resource for adipic acid production, as this renewable material is available at low-cost and in large quantities, but lignin-based routes are still largely unexplored.[11]

With lignin valorization in mind, catechol provides an interesting starting material. Indeed, guaiacols (*i.e.* catechol methyl ethers) are often reported as major products in lignin depolymerisation procedures[11–14] and hydrolysis may then afford the corresponding catechols.[15–18] In addition, lignin depolymerisation procedures that directly yield catechols have recently been reported.[19]

The catechol-based route reported here (Fig. 1) is inspired by Nature, with 1,2-catechol dioxygenase enzymes, for instance, being able to convert catecholic substrates to *cis*,*cis*-muconic acids. This enzyme belongs to the class of intradiol catechol dioxygenases, which selectively cleave the carbon–carbon bond of 1,2-dihydroxybenzenes between the two hydroxyl functionalities, using molecular oxygen.[20–23] The enzyme

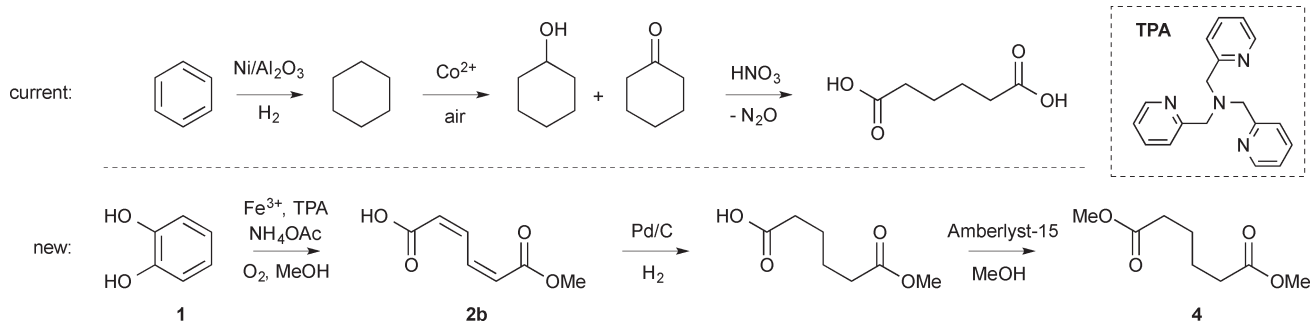

Fig. 1 The current industrial production of adipic acid starts from benzene, which is hydrogenated to cyclohexane. Aerobic oxidation using a cobalt catalyst affords KA oil, which is oxidised by nitiric acid to adipic acid. Our novel route starts from pyrocatechol, which is oxidized to the corresponding muconic acid by the iron catalyst. Subsequent hydrogenation and transesterification affords dimethyl adipate.

active site consists of an iron(III) centre in a non-heme coordination environment, where the substrate binds to iron as a dianion.[24]

Biomimetic synthetic iron(III) complexes bearing nitrogen and oxygen donor ligands have been developed as functional models for these intradiol cleaving dioxygenases and are able to perform this reaction.[25–27] The best performing complex in the stoichiometric intradiol dioxygenation of the activated model compound 3,5-di-*tert*-butylcatechol is the system based on tris(2-pyridylmethyl)amine (TPA) reported by Que *et al.*[28] Recently, we communicated the first example of catalytic intradiol dioxygenation reaction of pyrocatechol using an iron(III) TPA complex as catalyst, albeit still with somewhat modest turnover numbers.[29]

Herein, we report our further investigation into this reaction, which enabled a 35-fold improvement in the turnover frequency of the catalyst. The reaction was shown to proceed at catalyst loadings as low as 0.1 mol%, while an increase in reaction pressure and temperature significantly increased activity with retention of the excellent selectivity towards the desired oxidative cleavage products. Based on DFT calculations we show that isomerisation of the products takes place as a secondary, uncatalysed, reaction through a lactonic transition state. Furthermore, we investigated the sequential convergent hydrogenation and transesterification of the obtained product mixtures to dimethyl adipate, using compatible reaction conditions and recoverable catalysts, minimising the amount of work-up and isolation required in the reaction sequence.

Compared to the current industrial route, our new route is highly atom-efficient: water, rather than nitrous oxide, is the only stoichiometric by-product and only two equivalents of hydrogen (compared to three in the industrial process) are necessary to obtain the final adipates. In contrast to the high temperatures and pressures required for benzene hydrogenation in the conventional route, dearomatisation here proceeds oxidatively and as a result all reaction steps can be run at mild temperatures and pressures. Furthermore, our process uses largely non-toxic reagents and catalysts. The route thus provides a sustainable alternative to dimethyl adipate production.

2. Results and discussion

The dioxygenation of pyrocatechol (**1**) using an *in situ* prepared iron(III) tris(2-pyridymethyl)amine (TPA) complex (Fig. 1) was investigated in a stainless steel batch autoclave equipped with reflux condenser to allow reactions to be run at elevated pressures and under continuous gas flow. In our previous communication[29] we already showed that the highest activities are obtained with iron(III) salts with non-coordinating anions, using mild bases; we therefore used readily available iron(III) nitrate nonahydrate as the iron source here. Variation of base concentration showed that the highest activity was obtained with two equivalents of base relative to the catalyst. In order to prevent undesirable side reactions, the (very) weak base ammonium acetate was employed. The TPA ligand is commercially available, but can also be conveniently prepared by a literature procedure.[30] In all oxidation chemistry, including industrially practiced processes, such as the cyclohexane oxidation step of the current adipic acid process, one should be aware of the potential fire and explosion hazards that result from the use oxygen and flammable organic compounds and solvents under pressure and elevated temperature. Therefore, all experiments were run using a 1 : 3 mixture of synthetic air and nitrogen, for a final oxygen concentration of 5 vol%. This is well below the limiting oxygen concentration for a methanol/oxygen system and thus outside the flammability range.[31]

A typical reaction proceeded for 4 h at 50 °C and 10 bar total pressure, using 0.5 mol% catalyst. Products were isolated from the reaction mixture by acidification with aqueous HCl to dissociate the iron complexes and subsequent extraction with diethyl ether. In all reactions, a maximum of six products was observed, which all derive from the selective intradiol dioxygenation of catechol (Fig. 2). Products that derive from ring cleavage with a different regioselectivity (*i.e.* extradiol dioxygenation) were not observed. Thus, due to the convergent nature of the subsequent hydrogenation and esterification steps, all six products are desired, as they will all be converted to dimethyl adipate.

The cyclic muconic anhydride, which is the initial product of the intradiol dioxygenation reaction, is not directly observed.[25,28]

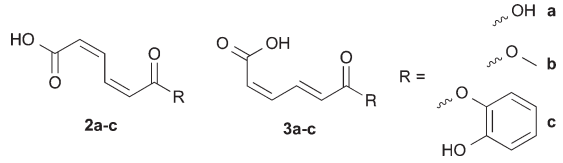

Fig. 2 Products observed in the catalytic dioxygenation of catechol are derivatives of *cis,cis*-muconic acid (**2**) and *cis,trans*-muconic acid (**3**). The products include free acids (**a**), methyl esters (**b**) and catechol esters (**c**).

Rapid nucleophillic attack by water, methanol or catechol affords, respectively, *cis,cis*-muconic acid (**2a**), its monomethyl ester (**2b**) and its catechol ester (**2c**). The major product observed in all cases is **2b**. At 96% conversion, a yield of 63% is observed, while yields of **2a** and **2c** are only 5% and 1% respectively. Isomerisation to the corresponding *cis,trans*-isomers (**3a–c**) is also observed, with a typical **2 : 3** ratio of 7 : 1.

The isomerisation of muconic acids has previously been proposed to proceed by intramolecular attack of the carboxylate moiety on the 1,3-diene to form a lactonic intermediate.[32,33] Given the rather mild conditions at which the reaction is performed, we used density functional theory (Amsterdam Density Functional, BP86 functional, TZP basis set) to check if such a mechanism would be feasible under our reaction conditions. Geometry optimisation of the monomethyl muconate anion indeed gave minima for the *cis,cis* and *cis,trans* isomers. As expected, the *cis,trans* isomer is the thermodynamic end product having a free energy that was slightly lower than the *cis,cis* isomer by 2.4 kcal mol^{-1}. Interestingly, however, no stable lactonic intermediate could be found, but increased lactonic character of the muconic acid did lengthen the carbon–carbon double bond. Consequently, we were able to optimise a lactonic transition state for the isomerisation (Fig. 3) with a free energy of 23.7 kcal mol^{-1} compared to

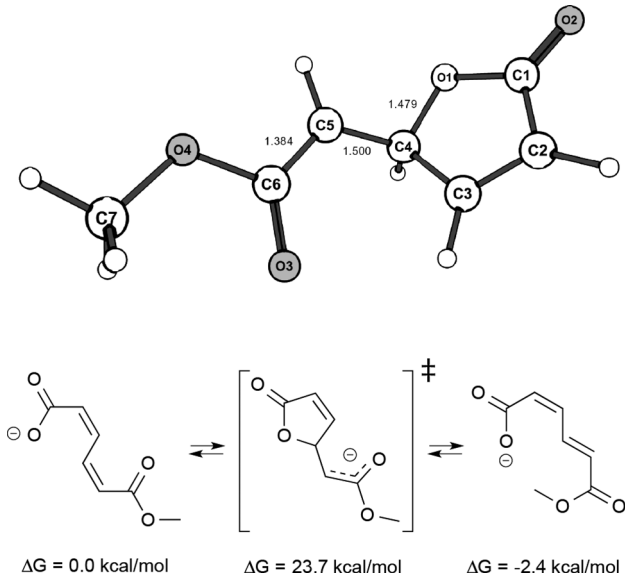

Fig. 3 Transition state (top, selected bond lengths indicated in Å) and mechanism (bottom) for double bond isomerisation in monomethyl muconate as revealed by density functional theory.

the *cis,cis* isomer. This appears to be a reasonable activation barrier considering the relatively low *cis,trans* isomer yields that are observed. In the dioxygenation of substituted catechols, lactones have previously been observed as products,[26,34,35] although we find none under our conditions. The absence of a lactonic intermediate also explains why no lactone products are observed, as these might otherwise be formed simply by protonation of such an intermediate.

Under standard conditions, the six products and unreacted catechol accounted for 99% of the original catechol. Under more severe reaction conditions, we were unable to completely close the mole balance (as moles of C_6-units found, against the original intake of C_6 units) and *ca.* 5–15% of the original catechol intake was unaccounted for. To ensure all muconate products were completely extracted from the reaction mixture, the aqueous fractions were analysed by UV-vis measurements after extraction. The muconate species have very intense absorption bands between 251 nm and 264 nm,[36] but no strong absorbances other than those from the TPA ligand could be observed (Fig. S7†). Having now excluded muconate losses due to the work-up procedure, we would attribute the reduced mole balance to noncatalytic oxidation to 1,2-benzoquinone, as we previously hypothesised. This highly unstable compound is known to undergo condensation reactions with catechol itself, forming poorly-defined, water-soluble oligomers, which are as a result not extracted and seen in our work-up procedure.[37–39]

2.1 Catalyst

As we have previously performed the intradiol dioxygenation at a rather high catalyst loading of 5 mol%, we were interested to see if the catalyst retained its activity at lower concentrations. Thus, the dioxygenation reaction was performed for 4 h of reaction time using loadings of 0.1–5 mol% catalyst at 50 °C and 10 bar total pressure (Table 1). At high catalyst loadings, the reaction proceeded with full conversion, while at lower catalyst loadings the turnover frequency increased up to 27 h^{-1} at 0.1 mol%. As the catechol intradiol dioxygenation proceeds approximately 0th order in substrate,[29] the increase in turnover frequency presumably is the result of the 0th

Table 1 Results of the catalytic dioxygenation of catechol using different amounts of catalyst[a]

	Cat.[b] (mol%)	Conv.[c] (%)	TOF[d] (h^{-1})	MB[e] (%)	Yield 2 + 3 (%)		
					a	*b*	*c*
1	0.1	12	27	99	1	10	<1
2	0.5	40	20	99	4	33	2
3	0.5[f]	43	18	93	3	28	4
4	1.0	90	19	91	6	61	7
5	2.0	100	10	92	4	71	10
6	5.0	100	8	86	3	64	9

[a] Conditions: 27.2 mmol catechol, catalyst (1 eq. $Fe(NO_3)_3$, 1 eq. TPA, 2 eq. NH_4OAc), 300 mL MeOH, 50 °C, 10 bar (5% O_2), 800 sccm gas flow, 4 h. [b] Catalyst loading. [c] Conversion. [d] Turnover frequency. [e] Mole balance. [f] Using iron(III) oxalate and no NH_4OAc.

order approximation being more valid at low conversions, rather than a true activity increase. The product distributions are largely unaffected by the concentration of the catalyst.

To further simplify the system and reduce the environmental footprint by omitting the externally added base, we were also interested in testing the activity of an iron(III) salt with weakly basic counterions. As the first turnover produces muconate anions which then in turn act as base to continue the catalytic cycle, the basic counter ions merely are needed to initiate the catalytic cycle and a pK_a ~3 of the conjugate acid should be sufficient. Thus, when performing the reaction using iron(III) oxalate (Table 1, entry 3) without any added base, an activity that was only slightly lower than with 2 eq. of NH_4OAc was obtained. The oxalate anions are also sufficiently basic to enable formation of the first catecholato complexes that initiate the catalytic cycle and also do not appear to significantly displace the catecholato moieties from the iron(III) centre.

2.2 Reaction pressure

In order to increase the activity of the system, the influence of the total gas pressure (5–25 bar at 5 vol% oxygen) was also investigated, using 0.5 mol% catalyst at 50 °C (Table 2). An approximately linear increase of activity with pressure was observed, suggesting a first-order process in oxygen. This is consistent with the proposed mechanism for catechol intradiol dioxygenation that involves attack of oxygen on the active iron catecholato complex[40,41] and with our recent mechanistic work on this system.[42] To exclude the influence of mass-transfer of oxygen into the liquid phase, which is also a first-order process, a control experiment with lower stirring rate was performed. The similar activity that was observed, together with the intrinsic low oxygen conversion (*ca.* 3%) in our experimental conditions, make it seem reasonable to assume that we are not working under mass-transfer limited conditions and that the pressure-dependent data represent the actual, expected order in oxygen. As with the catalyst loading, no significant changes in product distribution are observed with increasing pressure, which is also expected, as **2** and **3** are products of secondary reactions.

Table 2 Results of the catalytic dioxygenation of catechol using different total pressures (5% O_2).[a]

	p^b (bar)	Conv.[c] (%)	TOF[d] (h^{-1})	MB[e] (%)	Yield 2 + 3 (%)		
					a	***b***	***c***
1	5	29	11	96	2	18	2
2	10	43	20	99	4	33	3
3	10[f]	56	23	94	4	37	4
4	15	73	31	94	6	51	5
5	20	88	36	86	6	63	2
6	25	97	37	96	8	66	<1

[a] Conditions: 27.2 mmol catechol, 0.5 mol% catalyst (1 eq. $Fe(NO_3)_3$, 1 eq. TPA, 2 eq. NH_4OAc), 300 mL MeOH, 50 °C, 800 sccm gas flow, 4 h. [b] Pressure. [c] Conversion. [d] Turnover frequency. [e] Mole balance. [f] 400 rpm stirring.

2.3 Reaction temperature

The influence of temperature (30–80 °C) on the reaction was investigated at 10 bar total pressure (5% O_2) and 0.5 mol% catalyst (Table 3). As observed previously for the influence of catalyst loading and pressure, no significant changes in product selectivity were observed. Activities clearly increase with increasing temperature, although the mole balances do decrease somewhat with increasing conversion.

At first glance, the observed activities appear to increase approximately linearly with temperature, which is attributed to the rather narrow absolute temperature interval which was measured. To better interpret the dependence of the rate as a function of temperature, the data was plotted in the form of the Eyring–Polanyi equation (eqn (1), Fig. 4):

$$\ln\frac{k}{T} = -\frac{\Delta H^{\#}}{R}\frac{1}{T} + \ln\frac{k_b}{h} + \frac{\Delta S^{\#}}{R} \quad (1)$$

From the slope and intercept, the standard enthalpy and entropy of activation were determined to be 23.8 kJ mol^{-1}

Table 3 Results of the catalytic dioxygenation of catechol using different temperatures[a]

	T^b (°C)	Conv.[c] (%)	TOF[d] (h^{-1})	MB[e] (%)	Yield 2 + 3 (%)		
					a	**b**	**c**
1	30	21	8	94	1	14	0
2	40	45	16	90	3	25	4
3	50	43	20	99	4	33	2
4	60	75	28	84	4	45	5
5	70	84	30	76	7	53	0
6	75	96	35	75	5	62	2
7	80	96	40	87	8	69	3
8	80[f]	63	120	84	4	41	2

[a] Conditions: 27.2 mmol catechol, 0.5 mol% catalyst (1 eq. $Fe(NO_3)_3$, 1 eq. TPA, 2 eq. NH_4OAc), 300 mL MeOH, 10 bar (5% O_2), 800 sccm gas flow, 4 h. [b] Temperature. [c] Conversion. [d] Turnover frequency. [e] Mole balance. [f] 0.1 mol% catalyst, 25 bar pressure.

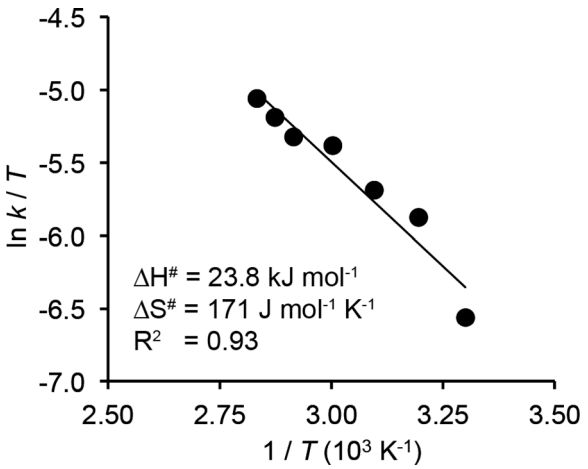

Fig. 4 Temperature dependence of the reaction rate of catechol intradiol dioxygenation expressed as an Eyring–Polanyi plot and the derived thermodynamic parameters.

and −172 J mol^{-1} K^{-1}, respectively. The large negative entropy of activation can be attributed to the binding of oxygen to the active catalyst complex, which is also not very favourable in terms of enthalpy and is thus an important limiting factor in the reaction rate. This high $\Delta S^{\#}$ is also in good agreement with our recent computational study on this system,[42] where we found an entropy of activation of −182 J mol^{-1} K^{-1}. Nevertheless, increasing the temperature from 30 °C to 80 °C afforded a five-fold increase in the reaction rate.

2.4 Improved conditions

Having investigated catalyst loading, pressure and temperature separately, we were also interested in obtaining maximal activity in the system. Combining a low catalyst loading (0.1 mol%) with high pressure (25 bar) and high temperature (80 °C), we were able to attain a TOF of 120 h^{-1} and a turnover number of 480 (Table 3, entry 8), which is a 35-fold improvement over our previously communicated system.

2.5 Hydrogenation and transesterification

For the investigation of the subsequent hydrogenation and transesterification steps to obtain dimethyl adipate, product mixtures were prepared from 3 g of catechol, using a standard oxidative cleavage condition, *i.e.* 4 h reactions with 0.5 mol% catalyst at 25 bar pressure and 80 °C to ensure full conversion of catechol. After isolation, a mixture of products is obtained as a solid in 85% yield (assuming an average molecular weight of 156.14), with full conversion and **3b** as the dominant product. As the hydrogenation and transesterification step converge all products to dimethyl adipate, no further separation of the products is required nor performed.

The hydrogenation reaction was investigated using commercially available catalysts. RANEY® nickel is a cheap and readily available hydrogenation catalyst, although often elevated temperatures and hydrogen pressures are necessary to obtain good activity. Nevertheless, we found that our mixtures were hydrogenated over RANEY® nickel at very mild conditions (16 h, 1 bar H_2, room temperature), although some half-hydrogenated muconic acid products (including the 3-ene isomer) were identified based on their ^{1}H NMR signals. After simple filtration to remove the catalyst, the ^{1}H NMR signals of the products were found to be extremely broad, suggesting the presence of paramagnetic species, possibly as Ni^{2+} carboxylates, in the sample. An additional acid wash step was thus required to obtain a clean hydrogenated mixture, after which the adipates were isolated in 57% yield.

A commercial palladium on carbon catalysts also readily hydrogenates the muconic acid mixture under the same mild conditions. Reflecting the higher activity of carbon-supported palladium, only fully hydrogenated products were obtained in near quantitative yield. As no half-hydrogenated products are observed in this case, this method is preferred for the hydrogenation. Nevertheless, in an industrial setting where more severe conditions to reach full conversion would not be limiting, the use of cheaper RANEY® nickel may be viable.

The transesterification of the hydrogenated acid mixture with methanol was previously successfully performed using *p*-toluenesulfonic acid as catalyst. Using a commercially available heterogeneous solid acid catalyst (Amberlyst-15) in refluxing methanol we were also able to (*trans*)esterify both free acids and catechol esters, to obtain dimethyl adipate. Purification by vacuum distillation (14 mbar, 80–105 °C) then affords highly pure dimethyl adipate in 62% overall yield. Analysis of the tarry distillation residue showed significant quantities of dimethyl adipate to be still present, which we were unable to recover given the rather small scale on which the distillation was performed. Furthermore, the distillation residue still contained the catechol liberated by transesterification of the catechol esters, which thus in principle could be recycled for another oxidation reaction.

Consequently, the main losses in the conversion of catechol to dimethyl adipate using our three-step route seem to occur by the radical oxidation of catechol during the first oxidation step, while hydrogenation and transesterification occur essentially quantitatively. Better recovery of the dimethyl adipate during the final step is rather a technical problem, which should be easily solved by better design of the distillation setup.

3. Experimental

3.1 Materials

Catechol (99+%) and iron(III) nitrate nonahydrate (98+%) were purchased from Acros. Ammonium acetate (HPLC grade) was obtained from Fisher Scientific. Iron(III) oxalate hexahydrate, 1-dodecanol (98%), RANEY® nickel (RANEY® 4200), palladium supported on carbon (5 wt% Pd) and Amberlyst-15 (dry, acid form) were obtained from Sigma Aldrich. Methanol (*p.a.* grade) was obtained from Merck. Compressed air (4.0) and nitrogen (5.0) were obtained from Linde Gas. All chemicals were used as received. Tris(2-pyridylmethyl)amine was synthesised according to a previously published procedure[30] and crystallised from boiling hexanes.

3.2 Physical measurements

NMR spectra were recorded on a Varian spectrometer operating at 400 MHz (^{1}H) or 100 MHz (^{13}C) in DMSO-d_6 (unless mentioned otherwise) and referenced against the signal of the residual protio impurity of the solvent (2.50 ppm). GC-MS measurements were performed on a Shimadzu GC-2010 using a VF5-ms column, coupled to a Shimadzu GCMS-QP2010 mass spectrometer.

3.3 Catalytic studies

Catalytic oxidation reactions were carried out in a fed-batch 500 mL stainless steel autoclave reactor setup (SA182-F316, rated up to 254 bar at 450 °C) by Autoclave Engineers. Gas inlet was controlled by Brooks mass flow controllers and gas outlet by a needle valve to maintain a constant pressure. The

effluent gas was cooled by a reflux condenser in order to minimise solvent losses.

In a typical experiment, the autoclave was charged with catechol (3.00 g, 27.2 mmol), aliquots of stock solutions of iron(III) nitrate (0.136 mmol), tris(2-pyridylmethyl)amine (0.136 mmol) and ammonium acetate (0.272 mmol), 1-dodecanol as internal standard (3.00 g, 16.1 mmol) and methanol (300 mL). The autoclave was sealed, purged with nitrogen and heated to a stable operating temperature. Oxygen was introduced by mixing compressed air with nitrogen (800 sccm gas flow, 5 vol% oxygen), marking the start of the reaction. After 4 h, gas flow was switched to pure nitrogen and the reactor was cooled to room temperature. A 1 mL sample was partitioned over 5 mL 1 M HCl and 5 mL diethyl ether. The organic layer was separated and the aqueous phase extracted two more times with 5 mL diethyl ether. The combined organic layers were dried over magnesium sulphate, filtered and concentrated *in vacuo*. The residual oil was dissolved in DMSO-d_6 and analysed by NMR spectroscopy. Products were quantified by their previously identified characteristic chemical shifts.[29] Turnover frequencies were determined by taking the total molar yield of intradiol cleavage and dividing by catalyst amount and reaction time. The k values (for use in the Eyring–Polanyi equation) were obtained by dividing the turnover frequency (in s^{-1}) by the oxygen concentration, which, based on Henry's law and the solubility of oxygen in methanol, was assumed to be 0.5 mM at 10 bar total pressure.[43]

Products for further hydrogenation and transesterification were prepared as above (at 80 °C and 25 bar pressure), but 1-dodecanol was omitted from the reaction mixture. After reaction, the methanol solution was concentrated to *ca.* 75 mL and partitioned over 100 mL 1 M HCl and 100 mL diethyl ether. The organic layer was separated and the aqueous phase extracted two more times with 100 mL diethyl ether. The combined organic layers were dried over magnesium sulphate, filtered and concentrated *in vacuo* to obtain 3.86 g of brown oil, which solidified upon standing (see Fig. S1† for a ^{1}H NMR spectrum).

In a typical hydrogenation experiment, the brown solid (3.86 g) obtained as above was dissolved in 50 mL methanol in a Schlenk flask under argon atmosphere. Palladium on carbon (5 wt% Pd, 0.203 g) was added and the flask brought at 1 bar hydrogen pressure by use of a gas balloon. After stirring for 16 h, the Pd/C catalyst was removed by centrifugation and filtration. The solution was concentrated *in vacuo* to obtain 3.82 g of brown oil, which based on the ^{1}H NMR spectrum (see Fig. S2†) consists exclusively of hydrogenated products.

In a typical transesterification experiment the oil as obtained above (3.82 g) was dissolved in 50 mL methanol. Amberlyst-15 (0.516 g) was added and the mixture refluxed for 22 h under nitrogen atmosphere. After cooling, the Amberlyst beads were removed by filtration and the solution concentrated to obtain a brown oil, which based on the ^{1}H NMR spectrum contained predominantly dimethyl adipate. Fractional vacuum distillation (14 mbar, 87–110 °C) afforded dimethyl adipate (2.92 g, 17.2 mmol, 62%) as a pale yellow oil (see Fig. S3–S5† for ^{1}H, ^{13}C and GC-MS analysis). ^{1}H NMR analysis of the tarry distillation residue (Fig. S6†) showed that it still contained a significant quantity of dimethyl adipate.

3.4 Computational methods

Density functional theory (DFT) calculations were performed with the Amsterdam Density Functional (ADF 2013.01) package,[44–46] using the BP86 functional[47,48] and the triple zeta Slater orbital basis set with polarisation functions (TZP) that is included with ADF.[49] Energies were corrected for solvation using the conductor-like screening model (COSMO)[50] and for dispersion interactions using Grimme's DFT-D3 dispersion correction[51] with Becke–Johnson damping.[52] All structures were subjected to geometry optimizations without any constraints followed by a full analytical frequency calculation. All reported structures were characterized by no (minima) or one (transition states) imaginary frequencies. Energies reported are Gibbs free energies at 298 K relative to the monomethyl *cis*,*cis*-muconate anion. Absolute energies for all structures are provided in the ESI.†

4. Conclusions

We have demonstrated the catalytic dioxygenation of catechol to derivatives of *cis*,*cis*-muconic acid using 5% oxygen in nitrogen, using a catalyst prepared *in situ* from iron(III) nitrate, tris(2-pyridylmethyl)amine and ammonium acetate. The reaction was shown to proceed at catalyst loadings as low as 0.1 mol% and activity was shown to be approximately linear with respect to oxygen. Investigating the temperature dependence of activity, a high entropy of activation was found, consistent with the need of oxygen to bind the active iron(III) catecholate complex. Nevertheless, an increase in temperature from 30 °C to 80 °C afforded a five-fold increase in reaction rate and a turnover frequency of 120 h^{-1} could be obtained.

Subsequent hydrogenation and transesterfication of the afforded muconic acid mixtures proceeded efficiently over commercially available hydrogenation and solid acid catalysts. After vacuum distillation, pure dimethyl adipate could be recovered in 62% yield from the catechol starting material, thus demonstrating a sustainable synthesis of this high volume nylon monomer.

To further improve dimethyl adipate yields, it will be important to reduce the amount of catechol lost to the non-productive radical oxidation. In addition, efficient separation and recycling of the iron catalyst, for example by heterogenisation, will enable a truly sustainable method for the production of dimethyl adipate.

Acknowledgements

P.C.A.B. acknowledges the Netherlands Organization for Scientific Research (NWO) for a Vernieuwingsimpuls Veni Grant. Dr. Rosa Bulo is acknowledged for providing access to

computational resources. The CatchBio program is acknowledged for financial support.

Notes and references

1 F. Cavani and S. Alini, in *Sustainable Industrial Chemistry*, Wiley-VCH Verlag GmbH & Co. KGaA, Weinheim, Germany, 2009, pp. 367–425.
2 A. Castellan, J. C. J. Bart and S. Cavallaro, *Catal. Today*, 1991, **9**, 237–254.
3 V. Hessel, I. Vural Gürsel, Q. Wang, T. Noël and J. Lang, *Chem. Eng. Technol.*, 2012, **35**, 1184–1204.
4 A. Castellan, J. C. J. Bart and S. Cavallaro, *Catal. Today*, 1991, **9**, 255–283.
5 R. A. Reimer, C. S. Slaten, M. Seapan, M. W. Lower and P. E. Tomlinson, *Environ. Prog.*, 1994, **13**, 134–137.
6 S. Van de Vyver and Y. Roman-Leshkov, *Catal. Sci. Technol.*, 2013, **3**, 1465–1479.
7 K. Sato, M. Aoki and R. Noyori, *Science*, 1998, **281**, 1646–1647.
8 M. Faber, *US Pat.* 4,400,468, 1983.
9 P. K. Wong, C. Li, L. P. Stubbs, M. van Meurs, D. G. Anak Kumbang, S. C. Y. Lim and E. Drent, International Patent Application WO 2012/134397 A1, 2012.
10 K. M. Draths and J. W. Frost, *J. Am. Chem. Soc.*, 1995, **117**, 2395–2400.
11 J. Zakzeski, P. C. A. Bruijnincx, A. L. Jongerius and B. M. Weckhuysen, *Chem. Rev.*, 2010, **110**, 3552–3599.
12 V. M. Roberts, V. Stein, T. Reiner, A. Lemonidou, X. Li and J. A. Lercher, *Chem. – Eur. J.*, 2011, **17**, 5939–5948.
13 J. Zakzeski, A. L. Jongerius, P. C. A. Bruijnincx and B. M. Weckhuysen, *ChemSusChem*, 2012, **5**, 1602–1609.
14 Q. Song, F. Wang, J. Cai, Y. Wang, J. Zhang, W. Yu and J. Xu, *Energy Environ. Sci.*, 2013, **6**, 994–1007.
15 A. Baeyer, *Chem. Ber.*, 1875, **8**, 153–155.
16 W. H. Perkin, *J. Chem. Soc., Trans.*, 1890, **57**, 587–589.
17 H. D. Dakin, H. T. Clarke and E. R. Taylor, *Org. Synth.*, 1923, **3**, 28.
18 S. B. Waghmode, G. Mahale, V. P. Patil, K. Renalson and D. Singh, *Synth. Commun.*, 2013, **43**, 3272–3280.
19 K. Barta, G. R. Warner, E. S. Beach and P. T. Anastas, *Green Chem.*, 2014, **16**, 191–196.
20 T. D. H. Bugg, *Tetrahedron*, 2003, **59**, 7075–7101.
21 F. H. Vaillancourt, J. T. Bolin and L. D. Eltis, *Crit. Rev. Biochem. Mol. Biol.*, 2006, **41**, 241–267.
22 M. Costas, M. P. Mehn, M. P. Jensen and L. Que Jr., *Chem. Rev.*, 2004, **104**, 939–986.
23 P. C. A. Bruijnincx, G. van Koten and R. J. M. Klein Gebbink, *Chem. Soc. Rev.*, 2008, **37**, 2716.
24 M. W. Vetting and D. H. Ohlendorf, *Structure*, 2000, **8**, 429–440.
25 D. D. Cox and L. Que Jr., *J. Am. Chem. Soc.*, 1988, **110**, 8085–8092.
26 W. O. Koch and H.-J. Krüger, *Angew. Chem., Int. Ed. Engl.*, 1995, **34**, 2671–2674.
27 R. Yamahara, S. Ogo, H. Masuda and Y. Watanabe, *J. Inorg. Biochem.*, 2002, **88**, 284–294.
28 H. G. Jang, D. D. Cox and L. Que Jr., *J. Am. Chem. Soc.*, 1991, **113**, 9200–9204.
29 R. Jastrzebski, B. M. Weckhuysen and P. C. A. Bruijnincx, *Chem. Commun.*, 2013, **49**, 6912–6914.
30 G. J. P. Britovsek, J. England and A. J. P. White, *Inorg. Chem.*, 2005, **44**, 8125–8134.
31 H. F. Coward and G. W. Jones, *Bureau of Mines Bulletin*, 1952, vol. 503, pp. 1–154.
32 B. M. Trost and P. G. McDougal, *J. Org. Chem.*, 1984, **49**, 458–468.
33 S. Seltzer and J. Hane, *Bioorg. Chem.*, 1988, **16**, 394–407.
34 M. G. Weller and U. Weser, *J. Am. Chem. Soc.*, 1982, **104**, 3752–3754.
35 M. Pascaly, M. Duda, F. Schweppe, K. Zurlinden, F. K. Müller and B. Krebs, *J. Chem. Soc., Dalton Trans.*, 2001, 828–837.
36 J. A. Elvidge, R. P. Linstead, P. Sims and B. A. Orkin, *J. Chem. Soc.*, 1950, 2235.
37 G. E. K. Branch and M. A. Joslyn, *J. Am. Chem. Soc.*, 1935, **57**, 2388–2394.
38 C. R. Dawson and J. M. Nelson, *J. Am. Chem. Soc.*, 1938, **60**, 245–249.
39 N. Schweigert, A. J. B. Zehnder and R. I. L. Eggen, *Environ. Microbiol.*, 2001, **3**, 81–91.
40 Y. Hitomi, M. Yoshida, M. Higuchi, H. Minami, T. Tanaka and T. Funabiki, *J. Inorg. Biochem.*, 2005, **99**, 755–763.
41 M. Higuchi, Y. Hitomi, H. Minami, T. Tanaka and T. Funabiki, *Inorg. Chem.*, 2005, **44**, 8810–8821.
42 R. Jastrzebski, M. G. Quesne, B. M. Weckhuysen, S. P. de Visser and P. C. A. Bruijnincx, *Chem. – Eur. J.*, 2014, **20**, 15686–15691.
43 C. B. Kretschmer, J. Nowakowska and R. Wiebe, *Ind. Eng. Chem.*, 1946, **38**, 506–509.
44 C. F. Guerra, *Theor. Chem. Acc.*, 1998, **99**, 391–403.
45 G. te Velde, F. M. Bickelhaupt, E. J. Baerends, C. Fonseca Guerra, S. J. A. van Gisbergen, J. G. Snijders and T. Ziegler, *J. Comput. Chem.*, 2001, **22**, 931–967.
46 ADF2013, SCM, Theoretical Chemistry, Vrije Universiteit, Amsterdam, The Netherlands, http://www.scm.com.
47 J. Perdew, *Phys. Rev. B*, 1986, **33**, 8822–8824.
48 A. D. Becke, *Phys. Rev. A*, 1988, **38**, 3098–3100.
49 E. Van Lenthe, *J. Comput. Chem.*, 2003, **24**, 1142–1156.
50 C. C. Pye and T. Ziegler, *Theor. Chem. Acc.*, 1999, **101**, 396–408.
51 S. Grimme, J. Antony, S. Ehrlich and H. Krieg, *J. Chem. Phys.*, 2010, **132**, 154104.
52 S. Grimme, S. Ehrlich and L. Goerigk, *J. Comput. Chem.*, 2011, **32**, 1456–1465.